

SINGLE PASS COLLIDER MEMO

DE84 013750

AUTHOR: H. SHOAEE, S. KHEIFETS

DATE: 7/11/84

REPLACES CN#

TITLE: Modification of the code BEAMCORR, and some simulation results of the magnet and achromat misalignments for the SLC South Arc

NOTICE

PORTIONS OF THIS REPORT ARE ILLEGIBLE. It
has been reproduced from the best available
copy to permit the broadest possible avail-
ability.

1.0 INTRODUCTION

This note supplements the previous note CN-252. Since the publication CN-252 an important decision has been made regarding the correction scheme for the arcs leading to the adoption of the so called scheme I. In this scheme the beam position data are collected from *single-plane* *x* and *y* BPMs, which are placed in the drift spaces adjacent to the downstream D- and F- magnets correspondingly. Similarly, *single-plane* *x* and *y* correctors are used for moving the upstream end of the corresponding magnets. In the present simulation this scheme is used exclusively.

The first order calculations performed by means of TRANSPORT appear to be unsatisfactory from the point of view of the beam spotsize at the interaction point (IP). In this note we describe the modification to our program BEAMCORR which employs second order calculations by means of the program TURTLE. We also present the results of the following simulations:

- a) study of the effects of two different levels of magnet misalignment on the beam spotsize at IP, and comparison of the results with those obtained by means of the program DINGBAT
- b) study of disjoints between achromats (both the displacement of the adjacent ends and angular discontinuity between achromats).

2.0 BEAMCORR2

The flow chart of the program is presented in Fig. 1. The input for the program is essentially the same as the input for the old version:

- a) the TRANSPORT input for the arc
- b) MMID table which specifies which magnets should be misaligned
- c) rms values and cutoff factors for the misalignments of dipoles, quads, sextupoles, and BPMs.

As in the original version of BEAMCORR, the initial step involves creating a TURTLE input file in which each misaligned magnet is sandwiched between two "7." cards representing displacements and tilts in horizontal and vertical planes. In addition, if radiation loss is required to be simulated, then the sixth parameter on each of the "7." cards represents half of the energy loss in a given magnet. The energy loss is restored to zero once per achromat, thus representing the tapering of the bending fields. To simulate achromat misalignment, each achromat as a

MASTER

whole is sandwiched by two additional "7." cards containing the corresponding Δz , $\Delta z'$, Δy and $\Delta y'$. Prior to correcting the orbit, the whole arc (excluding the Final Focus System) is divided into several segments which are then corrected consecutively. The flow chart for correction of an individual segment is presented in Fig. 2. The input file to the orbit correction step contains a list of the segments along with the position of correctors and monitors for each segment. Provisions have also been made to optionally permit correction of dispersion function at the end of each segment. Fig. 3 illustrates the flow chart for the dispersion correction algorithm.

The arc correction is followed by a separate 5-step orbit correction in FFS. The reasons for special treatment of FFS are the placement of BPMs inside the strong sextupole magnets and the lower misalignment tolerances in comparison with those for the arcs.

The final correction step takes place at IP where both the centroids and the dispersion functions are reduced to zero.

At the completion of the above correction steps the program **TURTLE** is used to trace one thousand rays through the whole system and collect the set of two dimensional histograms which represents the cross section of 6-dimensional phase space occupied by the particle trajectories at the IP.

A typical simulation of the South Arc, including the above corrections and the final ray tracing requires approximately 13 minutes of IBM 3081 CPU time. This time might however be decreased by proper segmenting of the arc. A reduction in the number of monitors and correctors per segment increases the number of steps, and hence the time required, linearly while decreasing the computation time for the individual steps quadratically.

3.0 SIMULATIONS

This section summarizes the results of correction scheme I as applied to the SLC South Arc with various errors and misalignments. All simulations were performed under the following conditions:

- All errors and misalignments have gaussian distributions and are truncated at $\pm 2.0\sigma$.
- 1000 rays were traced to obtain beam spotsize at IP.
- $\Delta p/p_0$ is truncated at $\pm 1.0\sigma$.
- There is no monitor misalignment at IP.

The following cases were investigated:

- a. Ideal machine: no synchrotron radiation(SR), errors or misalignments
(Table 1)
- b. SR; no errors or misalignments.
(Table 2)
- c. SR; magnet misalignment (100 μm)
(Table 3)
- d. SR; magnet & monitor misalignment (100 μm)
Fig. 4 presents a comparison of the results with those obtained from **DINGBAT**.
(Table 4)
- e. SR; magnet & monitor misalignment (200 μm)
(Table 5)

- f. SR; magnet & monitor misalignment (100 μm)
Achromat misalignment (100 μm)
(Table 6)
- g. SR; magnet & monitor misalignment (200 μm)
Achromat misalignment (200 μm)
(Table 7)

Table 1: Ideal Machine

- No errors, misalignments, or energy loss.

Run#	Seed	η corr. before FFS	σ_x μm	σ_y μm	$\frac{1}{\sigma_x \sigma_y}$ μm^{-2}
748	9876543	no	1.273	1.334	0.589

Table 2: Synchrotron Radiation

- Radiation energy loss
- No monitor or magnet misalignments

Run#	Seed	η corr. before FFS	σ_x μm	σ_y μm	$\frac{1}{\sigma_x \sigma_y}$ μm^{-2}
747	9876543	no	1.274	1.304	0.602

Table 3: SR, Magnet Misalignment

- Radiation Energy Loss
- Magnet Misalignment $100.0 \mu m$
- Quad Misalignment $70.0 \mu m$
- Quad Tilt Angle $60.0 \mu rad$
- No Monitor Misalignment
- No Achromat Misalignment

Run #	Seed	η corr. before FFS	σ_x μm	σ_y μm	$\frac{1}{\sigma_x \sigma_y}$ μm^{-2}
736	9234567	no	1.453	1.447	0.476
737	8234567	no	1.267	1.291	0.611
738	7234567	no	1.358	1.440	0.511
739	6234567	no	1.490	1.434	0.468
740	5234567	no	1.371	1.494	0.488
741	4234567	no	1.358	1.517	0.485
742	3234567	no	1.503	1.344	0.467
743	2234567	no	1.629	1.478	0.443
744	1234567	no	1.516	1.414	0.466
745	9876543	no	1.421	1.293	0.544

Table 4: SR; monitor and Magnet Misalignment ($100\mu m$)

- Radiation Energy Loss
- Magnet Misalignment $100.0 \mu m$
- Quad Misalignment $70.0 \mu m$
- Quad Tilt Angle $60.0 \mu rad$
- Monitor Misalignment $100.0 \mu m$
- Monitor Mis. in FFS $25.0 \mu m$
- No Achromat Misalignment

Run #	Seed	η corr. before FFS	σ_x μm	σ_y μm	$\frac{1}{\sigma_x \sigma_y}$ μm^{-2}	$\sum n^2$
850	9234567	no	1.501	1.650	0.404	4886
851	8234567	no	1.533	1.221	0.534	5610
852	7234567	no	2.213	2.207	0.205	2756
853	6234567	no	1.365	1.446	0.507	5445
854	5234567	no	1.487	1.436	0.468	5503
855	4234567	no	1.568	1.882	0.339	4019
856	3234567	no	1.984	1.817	0.283	4222
859	2234567	no	1.581	1.483	0.427	4584
858	1234567	no	1.916	1.908	0.274	4162

Table 5: SR; monitor and Magnet Misalignment (200 μm)

- Radiation Energy Loss
- Magnet Misalignment 200.0 μm
- Quad Misalignment 140.0 μm
- Quad Tilt Angle 120.0 μrad
- Monitor Misalignment 200.0 μm
- Monitor Mis. in FFS 50.0 μm
- No Achromat Misalignment

Run#	Seed	η corr. before FFS	σ_x μm	σ_y μm	$\frac{1}{\sigma_x \sigma_y}$ μm^{-2}	$\sum n^2$
780	3234567	yes	3.022	2.632	0.126	2783
790	4234567	yes	2.855	3.077	0.114	1843
784	5234567	yes	1.915	1.620	0.322	3956
793	6234567	yes	2.164	1.943	0.238	2978
792	7234567	yes	4.416	3.255	0.070	1258
782	8234567	yes	2.997	3.692	0.090	2560
783	9234567	yes	1.569	3.207	0.199	3105

- Monitor Mis. in FFS 20.0 μm

817	3234567	yes	3.062	2.018	0.162	3074
818	4234567	yes	2.792	2.715	0.132	2455
809	5234567	yes	1.693	1.532	0.386	4444
819	5234567	no	1.477	1.696	0.399	5075
814	6234567	yes	2.082	1.758	0.273	3302
813	7234567	yes	3.854	2.372	0.100	2140
815	8234567	yes	3.076	3.582	0.091	2802
816	9234567	yes	1.493	3.083	0.217	3318

Table 6: Achromat Misalignment (100 μm)

- Radiation Energy Loss
- Magnet Misalignment 100.0 μm
- Quad Misalignment 70.0 μm
- Quad Tilt Angle 60.0 μrad
- Monitor Misalignment 100.0 μm
- Monitor Mis. in FFS 25.0 μm
- Disjoints Between Achromats 100.0 μm
- Tilts Between Achromats 100.0 μm

Run#	Seed	η corr. before FFS	σ_x μm	σ_y μm	$\frac{1}{\sigma_x \sigma_y}$ μm^{-2}	$\sum n^2$
833	9234567	no	1.422	1.607	0.438	5004
834	8234567	no	1.694	1.260	0.469	5043
835	7234567	no	2.000	2.125	0.235	3246
836	6234567	no	1.392	1.543	0.466	5301
837	5234567	no	1.651	1.486	0.408	5118
838	4234567	no	1.652	1.851	0.307	3770
839	3234567	no	2.157	1.691	0.274	4085
840	2234567	no	1.683	1.319	0.450	5121

Table 7: Achromat Misalignment (200 μm)

- Radiation Energy Loss
- Magnet Misalignment 100.0 μm
- Quad Misalignment 70.0 μm
- Quad Tilt Angle 60.0 μrad
- Monitor Misalignment 100.0 μm
- Monitor Mis. in FFS 25.0 μm
- Disjoints Between Achromats 200.0 μm
- Tilts Between Achromats 200.0 μm

Run#	Seed	η corr. before FFS	σ_x μm	σ_y μm	$\frac{1}{\sigma_x \sigma_y}$ μm^{-2}	$\sum n^2$
849	9234567	no	2.029	2.101	0.235	3408
848	8234567	no	1.566	1.369	0.466	5531
846	6234567	no	2.184	2.386	0.192	3530
845	5234567	no	1.866	1.811	0.296	3875
844	4234567	no	1.984	2.006	0.254	3587
843	3234567	no	2.109	1.501	0.316	4272
841	2234567	no	1.790	1.289	0.433	5011

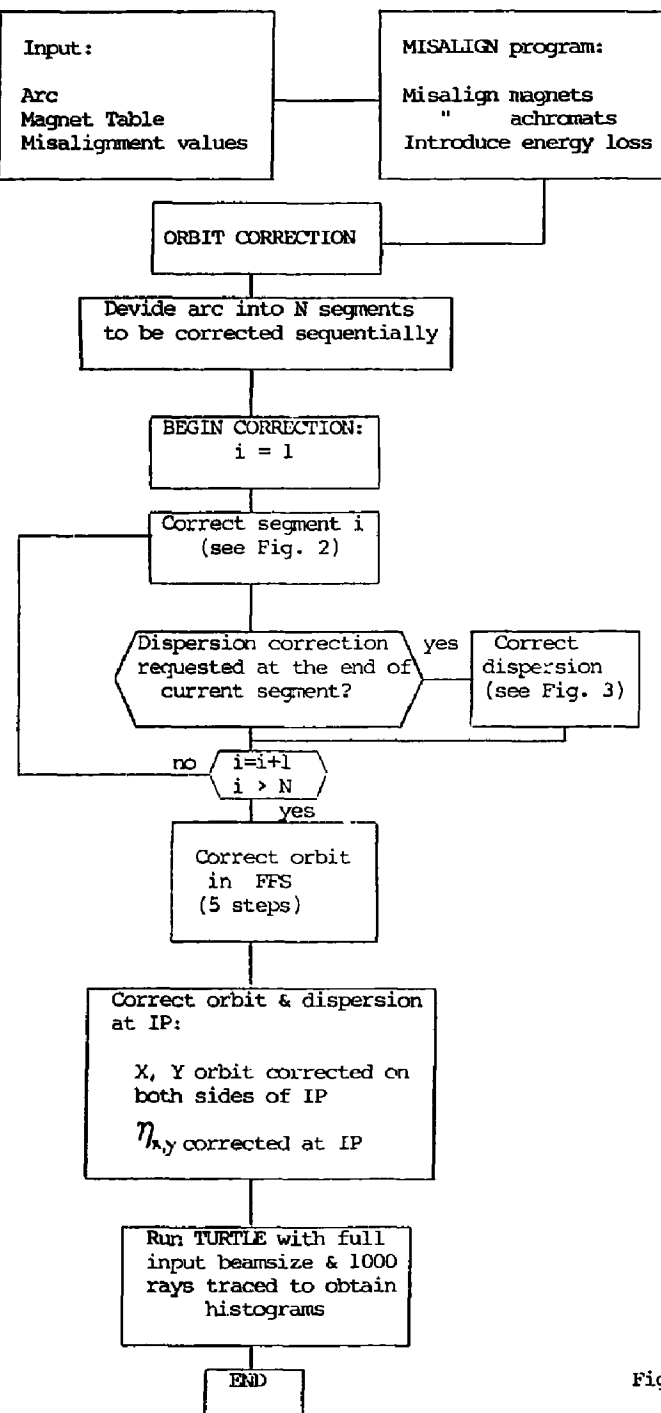


Figure 1

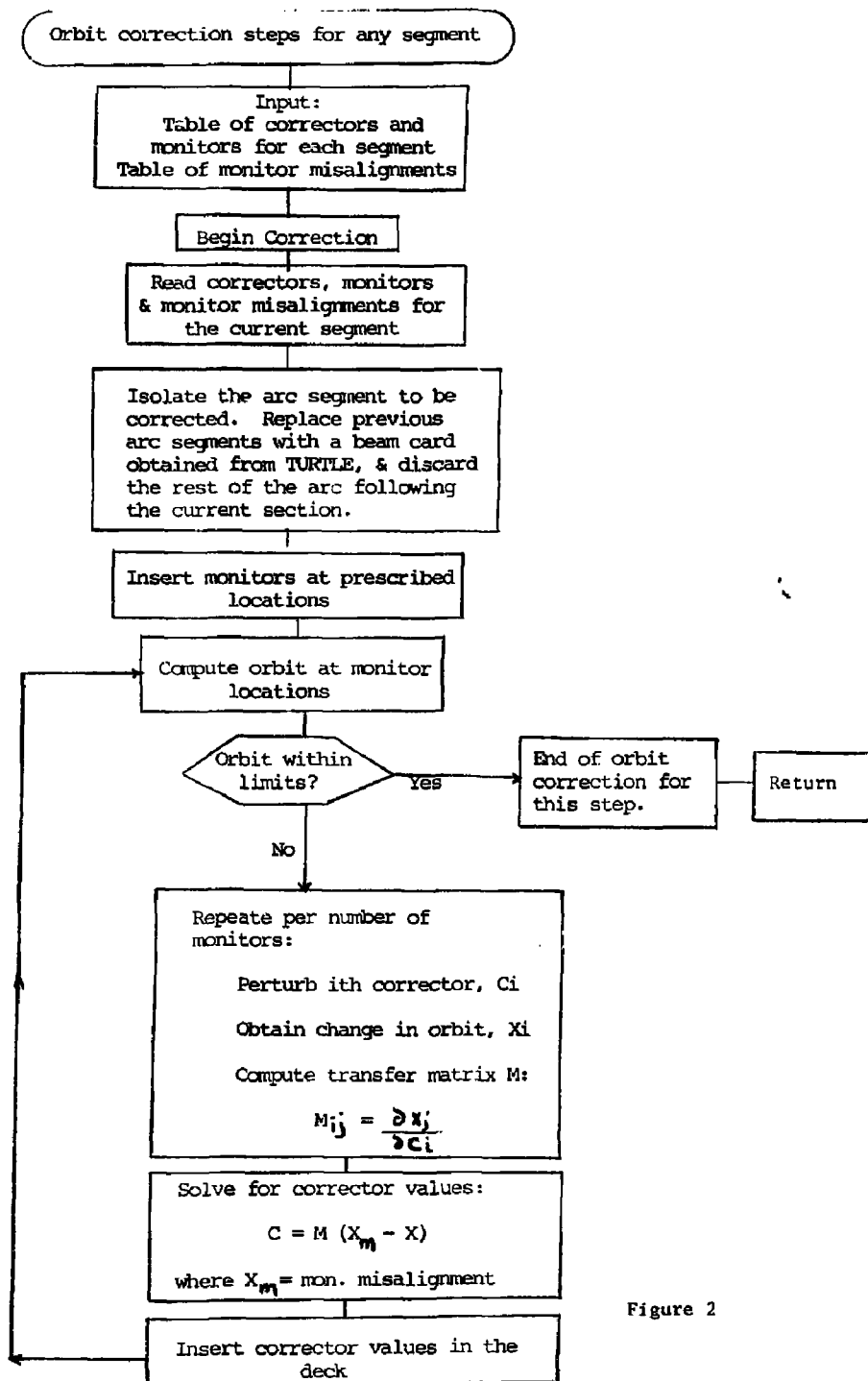


Figure 2

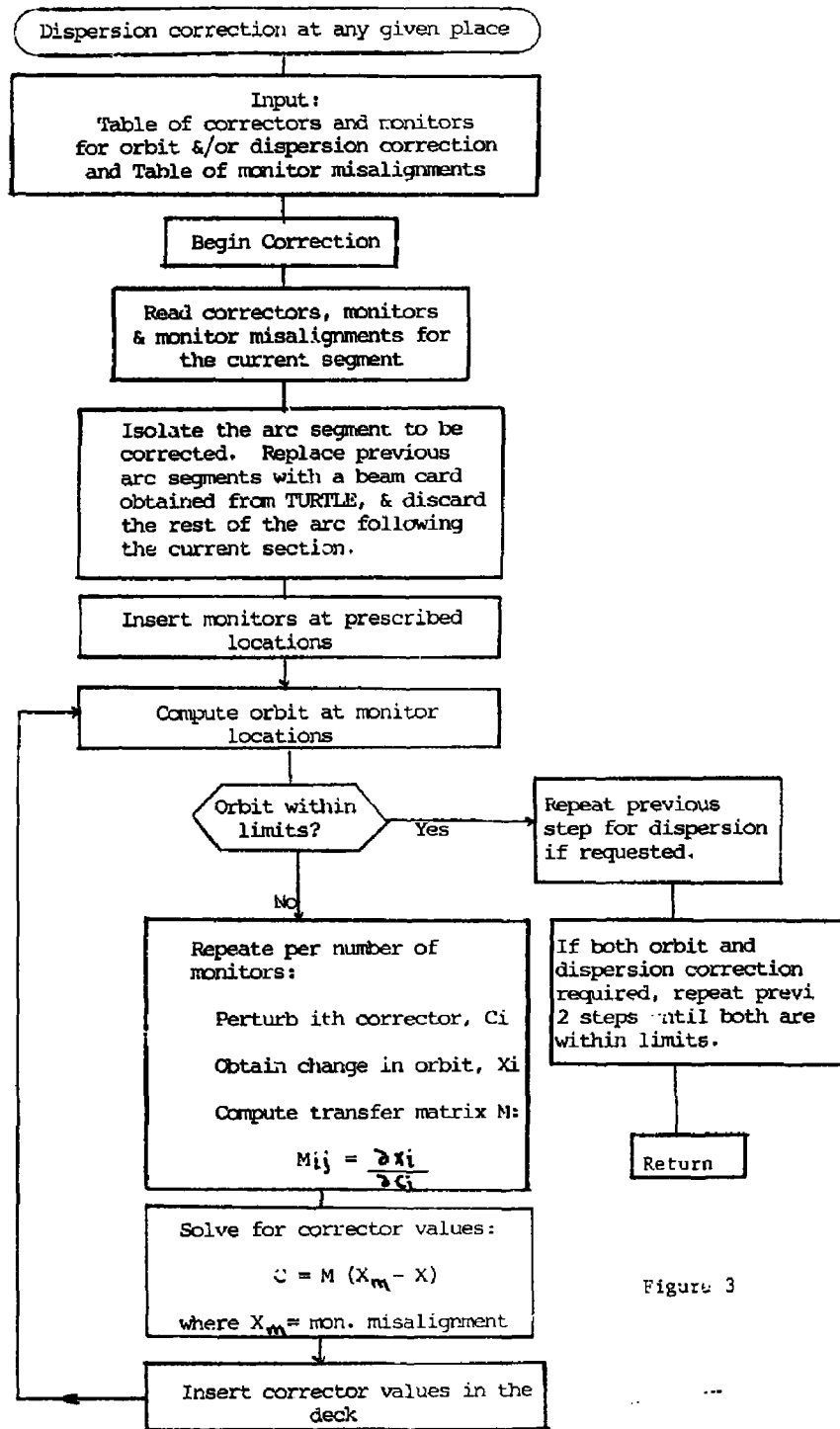
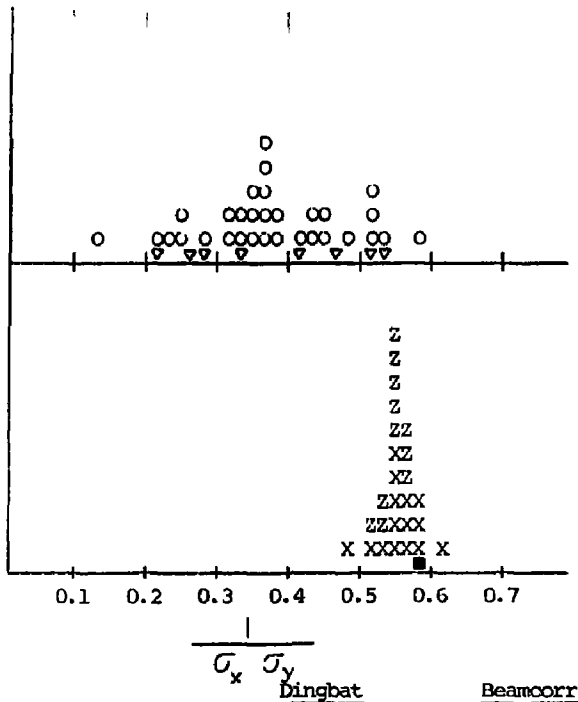


Figure 3

South Arc Simulation
with Dingbat & Beamcorr



σ_x σ_y
Dingbat

Beamcorr

Ideal South Arc (500) X

" " (1000) Z

Synch. Rad. O

Monitor Mis 100 mic V

Magnet Mis 100 "

Figure 4

SLAHO-0111-272

DISCLAIMER

This report was prepared as an account of work sponsored by an agency of the United States Government. Neither the United States Government nor any agency thereof, nor any of their employees, makes any warranty, express or implied, or assumes any legal liability or responsibility for the accuracy, completeness, or usefulness of any information, apparatus, product, or process disclosed, or represents that its use would not infringe privately owned rights. Reference herein to any specific commercial product, process, or service by trade name, trademark, manufacturer, or otherwise does not necessarily constitute or imply its endorsement, recommendation, or favoring by the United States Government or any agency thereof. The views and opinions of authors expressed herein do not necessarily state or reflect those of the United States Government or any agency thereof.

DISCLOSURE OF THIS DOCUMENT IS UNLAWFUL

QSL